



HAL
open science

RAMSEY FRINGES USING TRANSITIONS IN THE VISIBLE AND 10 μm SPECTRAL REGIONS: EXPERIMENTAL METHODS

Ch. Salomon, Ch. Bréant, Ch. Bordé, R. Barger

► **To cite this version:**

Ch. Salomon, Ch. Bréant, Ch. Bordé, R. Barger. RAMSEY FRINGES USING TRANSITIONS IN THE VISIBLE AND 10 μm SPECTRAL REGIONS: EXPERIMENTAL METHODS. Journal de Physique Colloques, 1981, 42 (C8), pp.C8-3-C8-14. 10.1051/jphyscol:1981801 . jpa-00221696

HAL Id: jpa-00221696

<https://hal.science/jpa-00221696>

Submitted on 4 Feb 2008

HAL is a multi-disciplinary open access archive for the deposit and dissemination of scientific research documents, whether they are published or not. The documents may come from teaching and research institutions in France or abroad, or from public or private research centers.

L'archive ouverte pluridisciplinaire **HAL**, est destinée au dépôt et à la diffusion de documents scientifiques de niveau recherche, publiés ou non, émanant des établissements d'enseignement et de recherche français ou étrangers, des laboratoires publics ou privés.

RAMSEY FRINGES USING TRANSITIONS IN THE VISIBLE AND $10 \mu\text{m}$ SPECTRAL REGIONS : EXPERIMENTAL METHODS[†]

Ch. Salomon, Ch. Bréant, Ch. J. Bordé and R.L. Barger (*) (**)

Laboratoire de Physique des Lasers, associé au C.N.R.S. n°282, Université Paris-Nord, F-93430 Villetaneuse, France

() Laseangle, Inc., Rollinsville, Colorado 80474, U.S.A. and Laboratoire de Physique des Lasers, Université Paris-Nord, F-93430 Villetaneuse, France*

Abstract. - A description is given of the experimental system which was used for obtaining Ramsey fringes with an atomic beam for the Ca 657 nm line, and for the system which is being set up to obtain fringes with a large absorption cell for various molecules in the $10 \mu\text{m}$ region. Details of the cat's eye and segmented retroreflector optical systems are discussed. Results obtained with Ca include fringe widths as small as 1 kHz HWHM, resolution of the recoil splitting, and resolution of second-order Doppler broadening and shift. The experiment at $10 \mu\text{m}$ is in progress and has already yielded a 1.25 kHz linewidth (HWHM) for the single zone signal with the SF_6 molecule.

Introduction. - The optical Ramsey fringe technique has been developed over the last few years to the point where extremely high resolution can now be obtained. Fringes have been observed for several atoms and molecules, including Ne (by Bergquist, Lee and Hall^{1,2}), CH_4 (by Bergquist,³ by Kramer,⁴ and by Baba and Shimoda⁵), Ca (by Barger, Bergquist, English and Glaze^{6,7,8}, and by Helmcke et al.,¹⁵), and SF_6 (by Bordé et al.,¹⁶). The use of this technique in investigations of the Ca 657 nm line at the National Bureau of Standards has produced linewidths as narrow as 1 kHz HWHM. This resolution has resulted in 1) complete resolution of the 23 kHz recoil splitting, 2) observation of the power contraction of this splitting, and 3) resolution of the second-order Doppler broadening and shift (1.7 kHz) and the attendant resolution-dependent distortion and shift of the Ramsey fringe profile. Experiments using the Ramsey technique in the $10 \mu\text{m}$ region with OsO_4 are now under way at the Laboratoire de Physique des Lasers. The experimental parameters should yield linewidths of less than 100 Hz and result in resolution of the superfine and hyperfine structures present in the $10 \mu\text{m}$ region spectra of many molecules. In this paper we shall discuss some of the experimental techniques which have been used in the visible and $10 \mu\text{m}$ experiments.

Ca : Experiment

The calcium atomic beam and fast-stabilized dye laser system used in this experiment (Fig. 1a) are described in detail elsewhere.^{2,9} Briefly, the $\text{Ca } ^1\text{S}_0 - ^3\text{P}_1$, $m_j = 0 \Rightarrow m_j = 0$ transition was excited in three standing-wave excitation zones with a laser beam of mode radius $w = 0.18$ cm. The dye laser frequency was stabilized to have short-term rms noise of about 1 kHz and long-term drift of less than 2 kHz/h. The total separation $2L$ of the three excitation zones was varied up to 21 cm, and the signal obtained by detecting fluorescence from a region about 10 cm downstream.

[†] Work supported in part by DRET, NBS, C.N.R.S. and NATO

(**) The research on Ca was done while this author was a member of the National Bureau of Standards, Boulder, Colorado.

In order to produce Ramsey fringes, the laser beams in the three zones must have wavefronts parallel to a small fraction of a fringe and must have their relative phases constant in time. (Since these phases determine whether the fringe intensity is positive or negative, random phase fluctuations will cause the fringe intensity to average to zero). These conditions were met in the experiment where the first observation of optical Ramsey fringes was achieved by J.L. Hall and his colleagues,¹ as well as in the early experiments⁶ on Ca, by the use of two opposing cat's eye retroreflectors as indicated in the circled insert of Fig. 1a. With the cat's eyes properly focused and free of aberrations three beams are obtained which are essentially portions of a "single plane wave", thus satisfying the requirements of parallelism and constant relative phases.

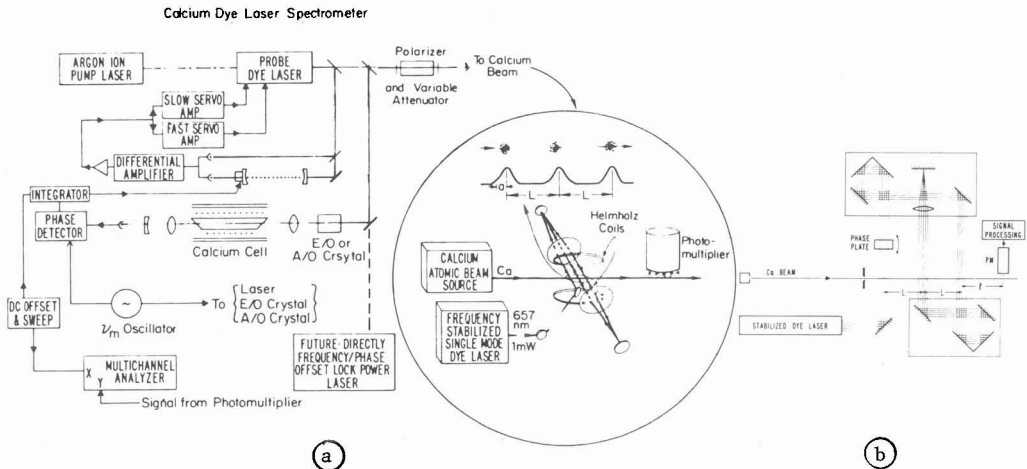


Figure 1

Experimental system for Ca. a) Stabilized laser and cat's eye optical system.
b) Segmented retroreflector optical system.

The opposing cat's eye system also has the beautiful and very important property, commonly called the "pulley effect," wherein the relative phases of the standing wave beams are not affected by changes in separation of the cat's eyes, changes caused by vibration, for instance. With a standing wave node formed at the reflection-surface of the central beam in the back cat's eye of Fig. 1a, the locations of the equal phase points in the three beams are determined by the distance from this node and for these "perfect" cat's eyes, lie on a straight line. If the upper cat's eye moves away from the lower one by a distance $+\delta$, the central beam phase point moves by $+\delta$, the right beam phase point by $-\delta$, and the left beam phase point by $+2\delta$. Thus the equal phase points still lie on a straight line, and, as long as the vibration periods are long compared to the atomic flight time, the fringe intensity is not changed.

In the early experiments with Ca, Ramsey fringes were obtained with opposing cat's eyes for beam separations $2L$ up to 7 cm. With the optics available to us, it was not possible to obtain wavefronts of good enough quality to produce Ramsey fringes for larger separations; thus, for higher resolution an interferometrically aligned segmented retroreflector (SRR) was developed.¹⁰ As can be seen in Fig. 1b the SRR consists of a corner cube to give retroreflection, two 45° mirrors (one adjustable in angle) to translate the retroreflected beam, and a small cat's eye or corner cube to retroreflect the central beam. A mechanically stable structure is obtained by mounting the corner cube and the adjacent 45° mirror on an Al block, the cat's eye on a second, and the other 45° mirror on a third, with the blocks rigidly mounted on ~ 3 cm diam Invar rods. To obtain long-term mechanical stability, most of the optical components are epoxied to the blocks. The final angular adjustment, very stable with time, is made by compressing three metal-metal contact points on the mount for the 45° adjustable mirror. The SRR offsets and retroreflects the incident laser beam so that the two beams are parallel to within a small fraction of a fringe over the mode diameter.

Two opposing SRR's form the three parallel standing wave beams for Ramsey fringes, as indicated in Fig. 1b. The input plane wave laser beam enters the first SRR at zone 1 in Fig. 1b and is retroreflected by it to zone 3. The beam is then retroreflected by the opposing SRR from zone 3 to zone 2, where it enters the central retroreflector of the first SRR. The beam is then retroreflected back around the optical circuit to produce the three standing-wave beams. The reflecting surfaces of the SRR's must be interferometrically aligned to obtain the required parallelism between input and reflected beams.

The first step in the interferometric alignment procedure is to obtain parallel laser beams (three in this case) with the desired spacing. These are then used to align the components of the SRR's. The experimental set-up is indicated in Fig. 2.

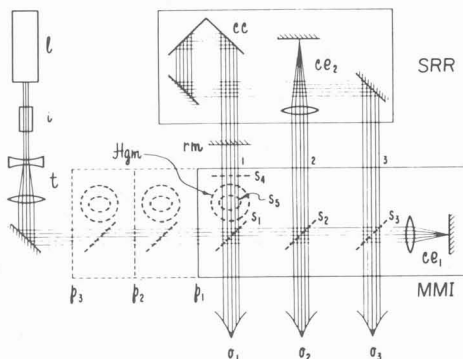


Figure 2

Interferometric alignment system

All components are mounted on a rigid tabletop. The components for obtaining the parallel beams are the input beam and small reference mirror rm , both fixed with respect to the table, and a modified Michelson interferometer (MMI), which can be translated parallel to the input beam. The input beam passes through optical isolator i and beam-expanding telescope t , which produces a plane wave of the desired mode diameter (~ 1 cm in this case). The MMI consists of flat beam splitters S_1 , S_2 , and S_3 (one for each desired beam, positioned to give the desired beam spacing), flat beam splitting end mirror S_4 , flat beam splitter S_5 , mercury reference mirror Hgm , and cat's eye or corner cube retroreflecting end mirror ce_1 . Beam splitter S_2 reflects a beam vertically down to mercury mirror Hgm , which forms a reflecting surface always in the horizontal plane. The Michelson components are mounted on a separate rigid platform that can be translated (without changing the mirror adjustment and rotated about the three orthogonal axes.

The interferometer is of the Michelson type but modified by replacing the plane end mirror in one of the arms with the retroreflector. This destroys the symmetry of reflections from the two arms and thereby greatly increases the sensitivity to relative changes of the angles between the input beam, the reflected beam, and the interferometer axis. This is seen from the following consideration. If the interferometer platform is rotated by angle θ , the angle of reflection from one arm changes by θ and that from the other by $-\theta$, resulting in localized fringes corresponding to the wedge 2θ . In contrast, for the normal Michelson with two flat end mirrors, the rotation would produce equal angles of reflection for the two arms, resulting in the relatively angle-insensitive circular fringe pattern. A fixed angular position of the Michelson platform is obtained by adjusting beam splitters S_1 , S_4 , and S_5 to give two uniform-intensity fringe systems at

observation point o_1 . These systems are formed by interference of the beams reflected from ce_1 and beam splitter S_4 and from ce_1 and horizontal reference mirror Hgm . The first system specifies the platform rotation about the two orthogonal axes perpendicular to the input laser beam, while the second specifies the rotation about the third orthogonal axis, that of the input laser beam. After these adjustments, the platform can be rotated, giving line fringes, and then returned to the original angular position by rotating the platform until the two uniform-intensity fringe systems are again obtained. If the fringe non-uniformity is detected visually to about 1/5 fringe, then the angular sensitivity of the platform rotation, for a 1 cm diam beam, is about 3×10^{-6} rad.

Much higher angular sensitivity can be obtained using electronic detection. An MMI has now been developed¹¹ which uses components corresponding to S_1 , S_4 and the retroreflector ce_1 in Fig. 2 together with a quadrant diode detector. This system has an angular sensitivity of a few times 10^{-12} rad for 100 s integration time, and has been used to servo the angle of a laser beam to be constant to about this level of precision.

The three output beams of the interferometer are made parallel by aligning all three normal to fixed reference mirror rm as follows. With the Michelson platform in position p_1 in Fig. 2, beam splitters S_1 , S_4 , and S_5 are adjusted to give the two uniform fringe systems at o_1 . Then reference mirror rm is placed in position to reflect output beam 1 and rotated until a uniform fringe is obtained at o_1 . Output beam 1 is now normal to the reference mirror, and the reference mirror at this angle is used for alignment of output beams 2 and 3.

To align beam 2, the Michelson platform and mercury mirror Hgm are translated to position p_2 (without changing the adjustment of S_1 , S_4 , or S_5) where beam 2 is incident on the reference mirror. The platform is rotated to give the two uniform fringe systems at translated observation point o_1 . Since the surface of the mercury reference mirror Hgm always lies in the horizontal plane, this rotation ensures that the angle of beam 1 is the same as for platform position p_1 (i.e., normal to the reference mirror). By now rotating beam splitter S_2 to give a uniform fringe at o_2 , beam 2 is made normal to the reference mirror and parallel to beam 1. By translating the platform to p_3 , beam 3 is made parallel to beam 1 with the same procedure. In this way, the three plane wave laser beams are obtained with all the wave fronts parallel. With the reference mirror removed, these beams can now be used for alignment of the SRR.

For interferometric alignment of the SRR, it is placed in the position indicated in Fig. 2 to give superposition of the reflected and input beams. By rotation of the adjustable 45° mirror in the SRR, the fringe systems at o_1 and o_3 can be made to have uniform intensities. This condition insures that an input plane wave at 1 is retroreflected at 3 as a plane wave parallel to the input beam. The central retroreflector at position 2 insures that the reflected beam 2 is parallel to input beam 2.

The "pulley effect," just as for the cat's eye system, preserves the relative phase relationships between the three beams if there is relative motion between the SRR's. With thermal drifts of the SRR's, however, the optical paths of beam 2 and of the offset beam change differently within the SRR, and this produces changes in the relative phases. Thus it would be desirable to reduce thermal drifts by making the SRR mounting blocks from Invar; however, even with the aluminium blocks used here, relative phase changes of $< \pi$ over periods of several hours have been achieved for a beam offset of 21 cm by placing each reflector in a nearly airtight insulating box.

Ca : Results

Let us first recall the simplified expression for the lineshape derived in the low field limit with a 4th order perturbation approach.¹⁴

The velocity distribution of atoms per unit volume is written :

$$F(\vec{r}, \vec{v}) = \frac{4 v^2}{\sqrt{\pi} u^3} \exp\left(-\frac{v^2}{u^2}\right) A(n_y, n_z, x, y, z) \quad (1)$$

where A is a function describing the angular distribution of the unit vector $\hat{n} = \frac{\vec{v}}{v}$; For a cell, A is a constant and for a beam in the x direction it is a very slow function of x .

The complex representation of the laser field propagating in the z direction is written

$$\begin{aligned} \vec{E} = & \sum_{\pm} (\hat{e}_1^{\pm} E_1^{\pm} G_1^{\pm}(y) G_1^{\pm}(x+L) e^{i\phi_1^{\pm}} \\ & + \hat{e}_2^{\pm} E_2^{\pm} G_2^{\pm}(y) G_2^{\pm}(x) e^{i\phi_2^{\pm}} \\ & + \hat{e}_3^{\pm} E_3^{\pm} G_3^{\pm}(y) G_3^{\pm}(x-L) e^{i\phi_3^{\pm}}) \exp(i\omega t \mp ikz) \end{aligned} \quad (2)$$

where \hat{e}_j^{\pm} is the polarization unit vector, G_j^{\pm} is the Gaussian distribution of each laser beam with waist w_0 , E_j^{\pm} and ϕ_j^{\pm} are the respective amplitudes and phases of the six fields. The fringe signal expressed as the power absorbed in units of quanta $\hbar\omega$ is :

$$\begin{aligned} \frac{\bar{W}}{\hbar\omega} = & -4\pi^2 \left[\Omega_3^- \Omega_2^- \Omega_2^+ \Omega_1^+ \left(\frac{w_0}{u}\right)^4 \right] \cdot \Phi_{\text{eff}} \\ & \text{(excitation efficiency)} \quad \text{(effective flux)} \\ & \times \text{Re} \int_0^{+\infty} \frac{dv}{v} \exp\left(-\frac{v^2}{u^2}\right) \exp\left(-2 \gamma_{\text{ba}} \frac{L}{v}\right) \\ & \text{(effective velocity distribution)(relaxation)} \\ & \times \exp\left[-\frac{(\omega - \omega_0)^2}{2v^2} w_0^2\right] W\left(\frac{w_0}{\sqrt{2}v} (\omega_0 - \omega)\right) \\ & \text{(envelope)} \\ & \times \exp\left[i(\phi_3^- - \phi_2^- + \phi_2^+ - \phi_1^+)\right] \exp\left[-i \frac{(\gamma\omega - \omega_0 + \delta)}{v} 2L\right] \\ & \text{(phases)} \quad \text{(oscillating term)} \end{aligned}$$

+ 3 similar terms obtained by exchanging $+\rightarrow-$ and $\delta \rightarrow -\delta$

$\Omega_j^\pm = \mu E_j^\pm / 2\hbar$ are the Rabi pulsations (see reference 19 for more detailed expressions taking the polarization into account); $\gamma = (1-v^2/c^2)^{-1/2}$ accounts for the transverse Doppler effect and 2δ is the recoil splitting; γ_{ba} is the decay constant of the optical coherence and W is the probability function for complex argument.

For beam experiments, if there is a decay of the upper level population with a relaxation constant γ_b , between the last zone and the detection region bounded by (l_1, l_2) , the following extra-factor should be added in the v integral to obtain the signal :

$$\exp\left[-\gamma_b l_1/v\right] - \exp\left[-\gamma_b l_2/v\right] \tag{4}$$

The effective flux of atoms Φ_{eff} is given by :

$$\Phi_{eff} = \left[n_a^{(0)} \frac{u}{kw_0} \int dy dz dn_y G^4(y) \exp\left(-2n_y^2 \frac{L^2}{w_0^2}\right) A(n_y, n_z = 0, y, z) \right] \tag{5}$$

This expression allows direct comparison between cell and beam experiments.

The results obtained with the experimental apparatus described above will now be briefly discussed. The separate Ramsey fringe patterns of the recoil doublet, split by 23 kHz, have now been completely resolved^{6,7} using beam separations up to $2L = 21$ cm, as is shown in the comparison of experimental and theoretical profiles in Fig. 3. The curves in the figure also show the influence of second-order Doppler

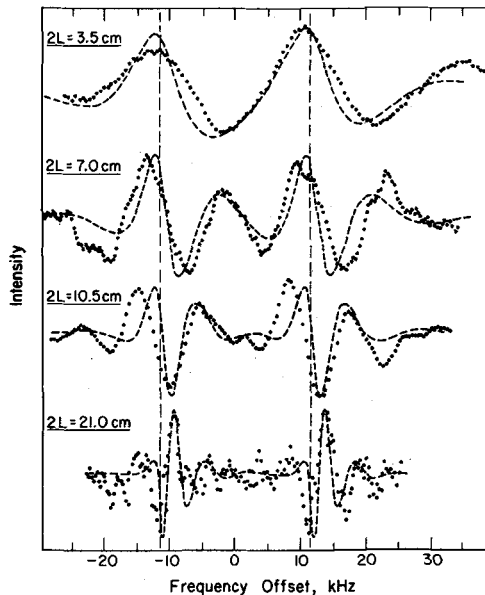


Figure 3

Comparison between experimental (...) and theoretical (----) optical Ramsey fringe profiles

broadening and shift on the Ramsey fringe profiles⁸ as resolution is increased from $2L=3.5$ cm, where the ratio of fringe width (FWHM) to second-order Doppler shift (1.7 kHz for $v=u$) is about 3, to $2L=21$ cm, where the ratio is about 1/2. This influence is clearly illustrated in the computer-generated contour plot of Fig. 4,

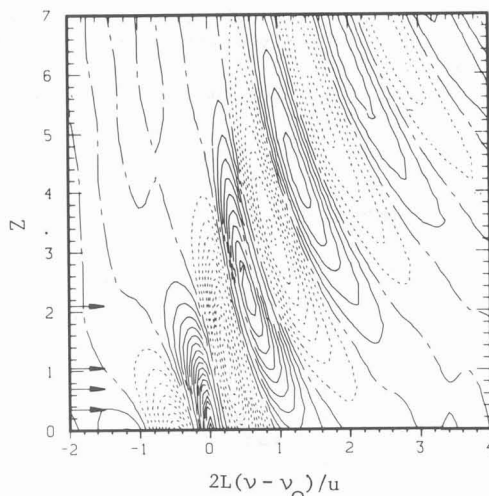


Figure 4

Contour plot of Ramsey fringe intensity versus normalized frequency $(v-v_0)/(u/2L)$ as a function of resolution. The resolution parameter Z is the ratio (FWHM of second-order Doppler distribution / FWHM of Ramsey fringe that would be obtained in the absence of the second-order Doppler shift). Contour interval, 5%. Intensities: —, positive; ---, negative; ···, zero.

which shows that with increasing resolving power the central fringe disappears as the first blue-side fringe builds up, then this first fringe disappears as the second builds up, etc. These effects are caused by the different-order dependence on atomic velocity v of 1) the second-order Doppler red shift, proportional to v^2 , and 2) the period of the Ramsey fringe for a single velocity proportional to v , as is seen in the following.

The frequency of the intensity maximum of the N th side fringe for a single velocity v is $v-v_0 = (Nv/2L) - v_0 v^2/2c^2$. With high resolution (and/or high velocity), the second term, the second-order Doppler shift to the red, becomes important. As v increases, the fringes on the red side of line center (negative N) and the central fringe ($N=0$) shift monotonically to the red, and integration over v makes these fringes broaden and integrate toward zero intensity. However, the fringes on the blue side (positive N) have the interesting characteristic of a linear shift to the blue with v and a quadratic shift to the red, and the slope of the total shift versus v curve changes sign for a turnaround velocity $v_t = Nc^2/2Lv_0$. With this turnaround, the N th fringes for velocities near v_t all occur at about the same frequency. If v_t is near u , integration over v can result in a strong and sharp fringe with a width much narrower than the second-order Doppler width.

In Fig. 3, the S/N is seen to be greatly degraded for $2L=21.0$ cm. With the optical Ramsey fringe technique, S/N should not be greatly reduced as resolution is increased,¹² and resolution of the second-order Doppler broadening should reduce the fringe height $(I_{\max} - I_{\min})$ by only about 10% for this value of $2L$, as seen in Fig. 4. Thus the degraded S/N is believed to be due to a combination of slight non-parallelism of the laser beams, residual laser-frequency jitter (the rms jitter is

approximately equal to the linewidth for this resolution), and, possibly, the recently measured angle jitter of our laser beam. The S/N degradation due to these effects could be reduced greatly as follows. The parallelism of the laser beams could be improved to the limit imposed by optics imperfections by use of a quadrant diode with the MMI alignment system to detect fringe uniformity. The frequency jitter could be reduced to a level of <100 Hz (less than the 400 Hz natural linewidth of the Ca line) by use of the recently developed sideband frequency servo techniques.¹³ Also, the angle jitter, which degrades the fringe intensity by introducing changes in the relative phases between the interaction zones during the atomic flight time, could be reduced to an uninteresting level with the angle servo interferometer.¹¹

An additional effect which we have observed is the power contraction of the recoil splitting predicted by Bordé.¹⁴ As power was increased, the splitting first contracted by about 2 kHz, and then with higher power expanded and then levelled off. The low power contraction fits fairly well with the low power limit of Bordé's 6th order theory which predicts the observed $\frac{\omega}{L}$ dependence. The theory for higher power is now being developed.

These results show that in order to achieve the ultimate line-center precision for this Ca line, it would be necessary to greatly reduce the Ramsey fringe power-dependent and resolution-dependent asymmetry and shift caused by the second-order Doppler shift. This can in principle be done,^{7,8} by either using velocity selection techniques or by laser cooling of the Ca beam. Systematic errors due to the power contraction of the recoil splitting can be reduced sufficiently through use of techniques discussed elsewhere.⁶

It should be possible to increase the present low S/N of the fringe signal to about 10^4 through use of photon-amplification techniques and optimization of the atomic beam design,⁶ leading to a pointing precision of about $\Delta v/v = 10^{-15} \tau^{-1/2}$, where τ is integration time. This high pointing precision should make it possible to correct systematic errors to better than 10^{-14} , giving a very high accuracy frequency standard in the visible spectrum.

10 μ m experiment

In spite of many theoretical works optical Ramsey fringes using 3 field zones in an absorption cell have been very little explored yet.^{3,5}

In order to keep a reasonable solid angle for molecules intersecting all three beams large diameter optical beams and correspondingly large retroreflectors have to be used. Such large retroreflectors have been made by optically contacting three $\lambda/10$ (in the visible) zerodur mirrors to form our 22 cm-aperture corner cubes with a $(5-10) \times 10^{-6}$ radians angular accuracy. After deposition of gold coatings, the junctions between faces were not visible.

The optical set-up is similar to the calcium experiment. The 10 cm-diameter folded standing wave with a beam spacing of $2L = 54$ cm is represented in Fig. 5. The two retroreflector structures (2, 3, 4, 5) and (5, 6, 7) are inside the large absorption cell and separated by 18 meters. The optics are mounted on massive aluminium blocks which are rigidly clamped to four Invar rods of 4 cm diameter to define the beam spacing L and to reduce thermal phase drifts between the three excitation zones. Phase modulation of the fringes can be achieved with PZT ceramics located under the 3 mounting points of corner cube n° 2. Helmholtz coils and a solenoid reduce the earth magnetic field inside the cell to less than 10% of its value. The three beams are made parallel within a small fraction of a fringe at 10 μ m with a multiple beam interferometer similar to the one described above for the Calcium experiment. However this interferometer has a corner cube instead of the cat's eye Ce_1 of Fig. 2 and has optics large enough for a 70 mm aperture.

For the final parallelism adjustment, mirrors 3 and 7 in Fig. 5 are rotated by means of three stainless steel metal-metal deformation contacts.

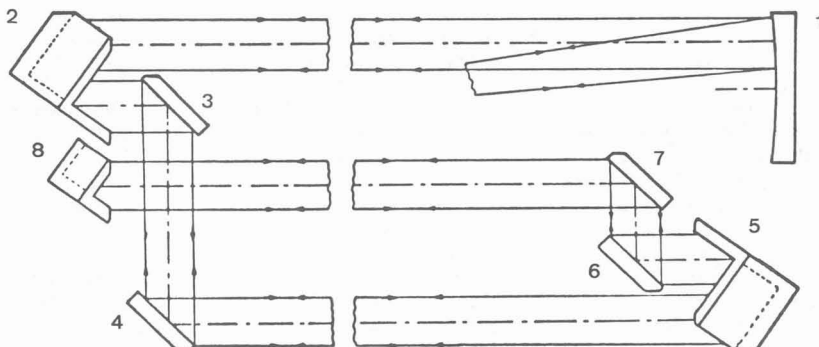


Fig.5 : Ramsey fringe optical set-up

optics diameter : 11 cm
 beam spacing : $2L = 54$ cm
 cell length : 18 m

As shown in Fig. 6, the output beam of a very stable frequency controlled CO_2 laser is expanded by a factor of ~ 7 to a $2w \sim 9$ cm with two confocal coincident-axis parabolas. The beam is spatially filtered by a pinhole of $800 \mu\text{m}$ diameter

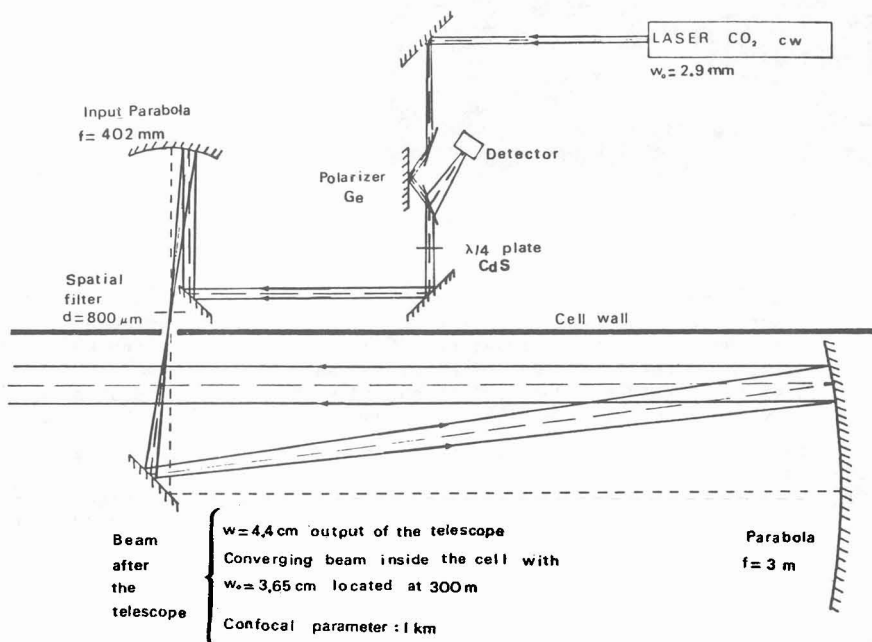


Fig.6 : Input optics for Ramsey fringe set-up

located at the telescope focus to produce an approximately Gaussian beam (within a few percent). Then by measuring the spot size of the beam at various distances (up to 54 meters), we have been able to determine the waist and curvature values shown in Fig. 6. Finally with the 10 cm diameter beam and the 1 km confocal parameter the wavefronts in the 3 zones are flat and parallel to about 1/10 of a fringe at 10 μm .

As a first test of the optical quality of this set-up, we have used the modified Villetaneuse spectrometer, to investigate the single zone saturated R(28)A₂^o line of the ν_3 band of ³²SF₆. Since the hyperfine structure of this line is well known,¹⁸ precise lineshape studies can be made.

A general diagram of this spectrometer can be found in these proceedings.¹⁷

Briefly, the CO₂ laser used for probing the large absorption cell is frequency-offset-locked from a second reference laser. This laser is in turn locked to a saturation line of a heavy molecule like OsO₄ obtained with a separate absorption cell using a line center 1st (or 3rd)⁴ derivative lock. Frequency tuning is accomplished through variation of the synthesizer frequency used in the frequency-offset-lock.

The stability of the lasers is illustrated in Fig. 7, which shows a spectral purity of ~ 150 Hz for the beat frequency of the two lasers locked independently to separate saturated absorption lines.

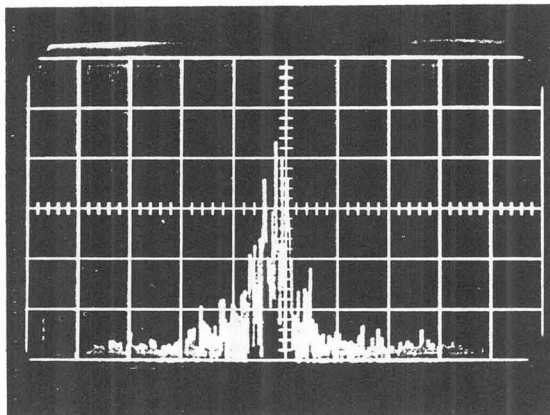


FIG.7 : Beat frequency spectrum of two CO₂ lasers locked to R(28)A_{2u}^o line of SF₆ and to a strong line of OsO₄. The frequency scale is 200 Hz/div. The vertical scale is linear and the resolution of the spectrum analyzer is 30 Hz.

This laser linewidth is of the order of the Ramsey fringe width (180 Hz FWHM) expected for our 54 cm beam separation for SF₆. With the lasers unlocked, the free running spectral purity is of the order of 1 kHz with drifts of a few kHz over several minutes. Also the same order of stability has been achieved with a waveguide CO₂ laser tunable over 500 MHz. This should provide a great deal of new hyperfine results for many molecules like SF₆, OsO₄, SiH₄, SiF₄, PF₅, NH₃ ...

This laser stability will be improved in the near future through acoustic isolation and better servo systems.

Fig. 8 shows the 1st derivative hyperfine spectrum of the R(28)A₂^o cluster of ³²SF₆ at 28.464 691 306 THz. The experimental linewidth is 1.2 kHz (HWHM). Also shown is the theoretical spectrum calculated by J. Bordé for the two overlapping I=3 (7 components) and I=1 (3 components) multiplets. The central three components are doublets with splittings of about 1.6; 1.1; 1.5 kHz. The linewidth is close to the value expected for our laser beam diameter as can be seen from the main contributions to the observed width (HWHM): geometrical effects: 650 Hz; collisions: 200 Hz; power broadening: 100 Hz; modulation broadening: 100 Hz; spectral purity of the laser: 100 Hz; residual Zeeman effect from the earth

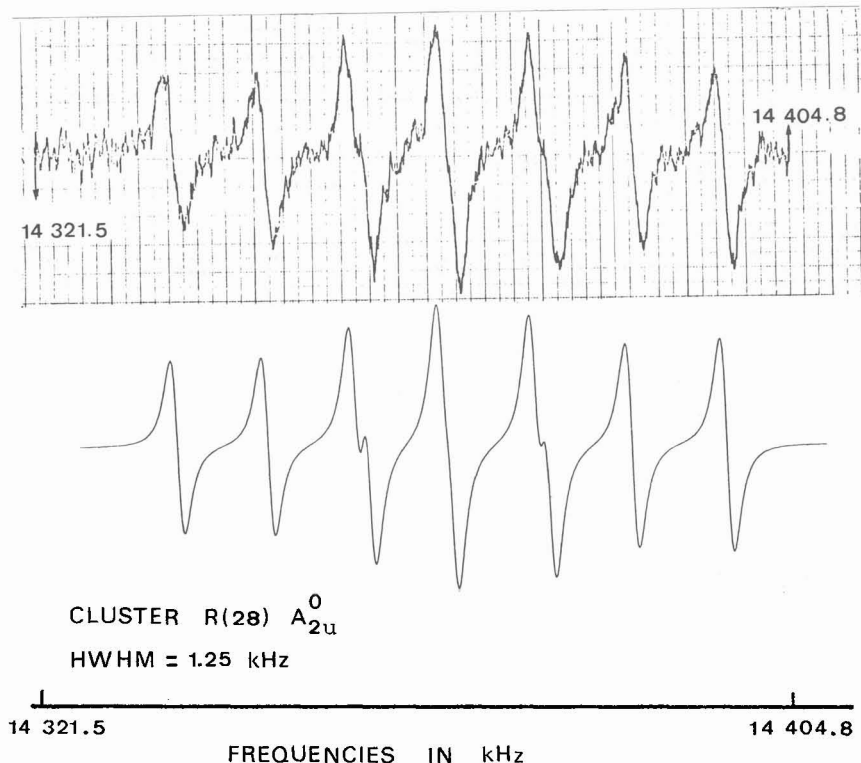


Figure 8

- Profiles of the R(28)A_{2u}⁰ line of the ν_3 band of $^{32}\text{SF}_6$.
- Upper : experimental first derivative spectrum (SF_6 pressure: 10^{-5} Torr; laser power: 4μ Watt; time constant: 1 s; sweep time: 5 min.)
 - Frequencies are in kilohertz from the $^{192}\text{OsO}_4$ line at 28 464 676 938.5 kHz
 - Lower : calculated profile (linewidth (HWHM) = 1.25 kHz).

magnetic field after compensation 20 Hz; other effects such as natural linewidth, recoil splitting, and 2nd order Doppler effect are also negligible.

In conclusion, we have presently reached the theoretical transit-time limited linewidth for single zone saturated absorption showing that the wavefronts are of good quality over the 11 cm optics diameter. We have demonstrated that open corner cubes can be used to produce good quality large infrared reflected beams and this is an important advance for high accuracy infrared saturation spectroscopy.

The next step will be to improve both the long-term stability of the lasers and the signal-to-noise ratio in order to detect the fringes.

References

- 1 BERGQUIST J.C., LEE S.A., and HALL J.L., Phys. Rev. Lett. 38, 159 (1977).
- 2 BERGQUIST J.C., LEE S.A., and HALL J.L., in Laser Spectroscopy III (Springer-Verlag, New York, 1977), p. 142.
- 3 BERGQUIST J.C., Ph. D. thesis (University of Colorado, 1978).
- 4 KRAMER G., J. Opt. Soc. Am. 68, 1634 (1978).
- 5 BABA M. and SHIMODA K., Appl. Phys. 24, 11 (1981).
- 6 BARGER R.L., BERGQUIST J.C., ENGLISH T.C., and GLAZE D.J., Appl. Phys. Lett. 34, 850 (1979).
- 7 BERGQUIST J.C., BARGER R.L., and GLAZE D.J., in Laser Spectroscopy IV (Springer-Verlag, New York, 1979), p. 120.
- 8 BARGER R.L., Opt. Lett. 6, 145 (1981).
- 9 BARGER R.L., WEST J.B., and ENGLISH T.C., Appl. Phys. Lett. 27, 31 (1975).
- 10 BARGER R.L., Appl. Opt. 19, 2088 (1980).
- 11 BARGER R.L., unpublished. This angle servo system is now commercially available from Laseangle, Inc., P.O. Box 223, Rollinsville, Colorado 80474, U.S.A.
- 12 BAKLANOV Y.V., DUBETSKI B.Y., and CHEBOTAYEV V.P., Appl. Phys. 9, 171 (1976). Also see ref.2 and SALOMON Ch., 3rd cycle thesis, Univ. Paris 13 (1979). In some experiments the Gaussian n_y dependence of the integrand in expression (5) of Φ_{eff} could also lead to a signal loss.
- 13 DREVER R.W.P., HALL J.L., KOWALSKI F.V., HOUGH J., FORD G.M., and MUNLEY A.J., Private communication.
- 14 BORDE Ch.J., in Laser Spectroscopy III (Springer-Verlag, New York, 1977), p. 121; and C.R. Acad. Sc. Paris, t. 284, 7 février 1977, Série B, p.101.
- 15 HELMCKE J., GLASER M., ZEVGOLIS D., YEN B.U., presented at third Symposium on Frequency Standards and Metrology, Aussois, France, October 1981.
- 16 BORDE Ch.J., AVRILLIER S., VAN LERBERGHE A., SALOMON Ch., BASSI D., and SCOLES G., presented at the Third Symposium on Frequency Standards and Metrology, Aussois, France, October 1981, and this issue.
- 17 CLAIRON A., VAN LERBERGHE A., BREANT Ch., SALOMON Ch., CAMY G., and BORDE Ch.J. in these proceedings.
- 18 BORDE J., J. de Physique Lettres, 39, L 175-178 (1978); BORDE Ch.J., OUHAYOUN M., and BORDE J., J. Mol. Spectrosc. 73, 344 (1978); BORDE Ch.J., OUHAYOUN M., VAN LERBERGHE A., SALOMON Ch., AVRILLIER S., CANTRELL C.D., and BORDE J., in Laser Spectroscopy IV (Springer-Verlag, New York, 1979) p. 142; BORDE J., BORDE Ch.J., SALOMON Ch., VAN LERBERGHE A., OUHAYOUN M., and CANTRELL C.D., Phys. Rev. Lett. 45, 14 (1980).
- 19 BORDE J., and BORDE Ch.J., J. Mol. Spectrosc. 78, 353 (1979).